Biosimulation of Normal Pressure Hydrocephalus Using COMSOL Multiphysics

K. Shahim[*,1], J.-M. Drezet [1], J.-F. Molinari [2], Sh. Momjian [3] and R. Sinkus [4]
[1] LSMX, Ecole Polytechnique Fédérale de Lausanne, Lausanne, Switzerland,
[2] LSMS, Ecole Polytechnique Fédérale de Lausanne, Lausanne, Switzerland,
[3] University Hospitals of Geneva and University of Geneva, Switzerland,
[4] Laboratoire Ondes et Acoustique, ESPCI, Paris, France
*Corresponding author: LSMX, Station 12, CH-1015 Lausanne, Switzerland, kamal.shahim@epfl.ch

Abstract: A numerical finite element model of one human brain is built in Comsol in order to study a particular form of hydrocephalus, the so-called normal pressure hydrocephalus (NPH). The geometry of the ventricles and the skull is obtained by magnetic resonance imaging (MRI) and imported in COMSOL Multiphysics. Form the mechanical point of view, the brain parenchyma is modeled as a porous medium fully saturated with the cerebrospinal fluid (CSF) using the Biot's theory of consolidation. Diffusion tensor imaging (DTI) is used to establish locally the direction of the bundles of neurons (fiber tracts). Novel ideas are introduced to link the diffusion with CSF permeability in brain. To find out the influence of the anisotropy in permeability, two models are tested under the same CSF pressure gradient. To remain coherent, the average properties over the brain parenchyma are the same in the two models.

Keywords: biomechanics, brain parenchyma, elasticity, permeability, anisotropy

1. Introduction

Normal pressure hydrocephalus (NPH) is a form of hydrocephalus and is one of the few treatable causes of dementia. In NPH, the ventricles enlarge although the CSF pressure remains close to normal within the ventricles [1-3]. The origin and the evolution of NPH are yet unclear compared to non-communicating or obstructive hydrocephalus which is caused by a CSF flow obstruction. NPH is generally categorized as a particular form of communicating hydrocephalus with the absence of any CSF-flow obstruction. The pathological manifestations of NPH are gradual memory loss (dementia), balance disorder (ataxia), urine incontinence and a general slowing of activity [2, 3]. The existence of NPH was first pointed out by Hakim and Adams in 1965 [3], who asserted that the pressure within ventricles is not solely responsible for the dilation of ventricles. In their work, the product of ventricular pressure and ventricular area were considered as an effective parameter to the possible explanation of NPH. Later on, more advanced analytical and numerical models were developed to try to understand the development of NPH. Elastic and poro-elastic models based on the Biot's theory of consolidation [4] have been used. All models assumed fully isotropic and homogenous elasticity and permeability properties within the brain parenchyma [2, 5-6]. Non-linearity has been introduced through either a dilation dependent Young's modulus or a dilation dependent permeability of the brain parenchyma [7, 8]. With the help of the finite element (FE) technique, different kinds of constitutive equations [1, 5, 7, 8 and 9] were introduced. Pena et al. [1,9] enlightened the influence of the ventricular geometry on increasing the intera-ventricular pressure using a FE model. By introducing nonlinearity such as large deformation theory and hyperelastic constitutive behavior in a 3D model of brain, Roy et al. [8] considered different cases such as compressibility of the solid part, single phase or biphasic models to understand NPH. By using a 2D isotropic model, Momjian et al. [5, 7] and Pena et al. [9] showed that the greatest stress concentrations and the largest deformations occur at the anterolateral angle of the frontal horn.

The brain parenchyma represents per se a heterogeneous medium and the presence of bundles of axons, i.e. fiber tracts, in the white matter gives birth to anisotropy in the permeability properties. On the other hand, the gray matter (neuron bodies) exhibits more isotropic properties. The influence of anisotropy

in permeability has never been studied numerically mainly owing to the absence of data. Abolfati [10] determined the anisotropic properties of brain white matter using a micromechanical model. Linninger et al. [11] simulated 3D CSF flow inside human brain numerically using CSF velocity data captured by Cine phase-contrast method. For the first time, three important elements in intracranial dynamics (brain, CSF, and blood) were considered. Nevertheless, the brain distortion and stresses have not been simulated in their models.

A transverse isotropic (TI) model, as described in Fig. 1, has been recently introduced by Larrat et al. [12] for the elastic property. Indeed, the elastic stiffness is higher along the fiber tracts than perpendicular to them. The direction of the fiber tracts is aligned with the (3) axis as shown in Fig. 1 and is given by diffusion tensor imaging, a non invasive technique. The plane perpendicular to this direction (plane (1,2) in Fig.1) is isotropic in elasticity.

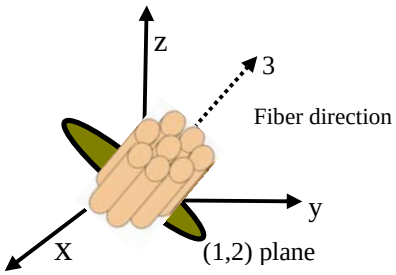

Figure 1: schematic representation of the fiber tracts direction (3) and the plane of isotropy (1,2) for the permeability [12].

The difficulty in studying medically NPH arises from the inaccessibility of brain tissue using invasive techniques. On the other hand, non-invasive techniques can provide us with precious data on the brain properties.

In the present investigation, the CSF permeability is assumed to exhibit the same transverse anisotropy as elasticity (cf. Fig.1). In other words, the permeability coefficients are different along the direction of the fiber tracts than perpendicular to them. In order to determine the direction of the fiber tracts in the white matter, DTI is used. Then for each voxel, the permeability tensor is expressed in the local frame (1,2,3). The goal of the present study is to assess the importance of a non-homogeneous and non-isotropic permeability in the CSF flow pattern within the brain parenchyma. To do so, voxel based results coming from non-invasive techniques such as MRI and DTI are used.

1.1 Magnetic resonance imaging (MRI)

MRI is used to determine the geometry of the brain parenchyma, i.e. of the space between the skull and the ventricles. Indeed, MRI is a well established medical imaging technique used in radiology to visualize the structure and function of the body because it yields excellent soft tissue contrast. It is possible to build sections or even 3D geometry of brain parenchyma using Comsol in connection with Matlab program from MRI images.

1.2 Diffusion tensor imaging (DTI)

The existence of fiber tracts accounts for the anisotropic CSF diffusion within parenchyma. It is possible to obtain the CSF self-diffusion tensor in the brain using DTI [13]. When this tensor is expressed in the fiber direction (local frame (1,2,3)), three eigen values D_1, D_2 D_3 and their corresponding eigenvectors are obtained. The mean diffusivity (MD) [m^2/s] and the diffusive fractional anisotropy (F_{AD}) [-] are defined respectively as:

$$\mathrm{MD} = \bar{D} = \frac{D_1 + D_2 + D_3}{3} \qquad [1]$$

$$\mathrm{F_{AD}} = \sqrt{\frac{3}{2}}\sqrt{\frac{(D_1-\bar{D})^2 + (D_2-\bar{D})^2 + (D_3-\bar{D})^2}{D_1^2 + D_2^2 + D_3^2}} \qquad [2]$$

Mean diffusivity (MD) is used to distinguish between cerebrospinal fluid (where MD is high) and brain tissue (lower MD). On the other hand, high fractional anisotropy (F_{AD}) indicates white matter because the directionality of the axon bundles permits faster diffusion along the neurons than across them [13].

DTI experiment was carried out on one human brain at the University Hospitals of Geneva. The MRI and DTI data of a given brain are considered as the base for the numerical calculation. The data are voxel based (size of voxel is $1.88\times1.88\times2mm^3$). The eigen vector of the diffusion tensor and the their two associated

invariants are used for each voxel as input for the numerical model in Comsol.

2. The Finite Element Model

The MRI data consists of 128×128×70 voxels in x, y and z direction respectively. The size of each voxel is 1.88×1.88×2mm^3. An axial slice of the geometry of the brain has been extracted using Matlab program connected to Comsol. Fig. 2 shows the top view of the domain and the associated mesh. In this slice, the two ventricles are visible and separated. The mesh is made out of 63'104 prism elements with 64'398 nodes.

Figure 2. 2D slice mesh of the brain parenchyma. The ventricles are not meshed.

A 2D work-plane is defined in the Comsol work-plane settings. Free mesh parameters are used to construct the required elements for this 2D work-plane. The size of each element is chosen so that it is lower than the voxel size. It is chosen in a way to include all the experimental voxel based data. The mesh is refined in the region close to ventricle walls. Finally, the mesh is extruded to the 3D computational domain. The thickness of the slice is chosen as 2 mm that is the height of the voxels. The voxel based data are interpolated between each finite element.

2.1 Constitutive equations

Brain parenchyma is modeled as a porous medium fully saturated with the CSF. The evolution of NPH being very slow (months or years), a steady state situation is assumed. The Biot's equations [4] for an incompressible fluid and completely saturated medium are summarized in the following equations assuming that there is no CSF sink or source term inside the parenchyma:

$$div(\boldsymbol{\sigma}) + \vec{\nabla} p = \vec{0} \quad [3]$$

$$\nabla \cdot (\mathbf{k}\vec{\nabla} p) = 0 \quad [4]$$

where $\boldsymbol{\sigma}$ is the effective stress tensor and p is the CSF pressure. The variable $\mathbf{k}$ denotes the permeability tensor (m^2) within parenchyma. The four unknowns of the problem are u_x, u_y, u_z, the three components of displacement of the solid constituent, and p the pressure of extracellular CSF, therefore there are four degrees of freedom per node.

Solid, stress-strain (smsld) and Poisson's equation (poeq) are coupled for modeling the multiphysics of the brain in the Comsol platform. In addition to the global coordinate systems, the fiber directions are constructed based on DTI eigen vectors. The new coordinate systems are aligned to the fiber direction to account for the local anisotropy. It is included in the model by providing Comsol the local (1,2,3) directions in each voxel.

The two coupled differential equations are solved by Comsol. Direct solvers are more accurate but high memory consuming. On the other hand, iterative solvers allow accessing and changing the memory efficiency and accuracy by trying different preconditioners. Among different types of iterative solvers in Comsol, GMRES with geometric multigrid preconditioner is used. Quadratic functions are used for both displacement and pressure in each element. In the calculation of deformation, small deformation theory is used.

2.2 Initial and boundary conditions

Initial conditions are taken as zero for displacements and stresses at all points. Initial pressure is zero. The calculation consists in finding the solution where the pressure within the ventricles is increased to 5 mmHg (i.e. 666.61 Pa) whereas it is kept to zero on the outer boundary (Dirichlet condition). The ventricles are permeable and they can deform freely. Therefore, the boundary condition on the ventricles is $\boldsymbol{\sigma} \cdot \vec{n} = -p\,\vec{n}$ with $p = 5$ mm Hg where $\vec{n}$ represents the normal vector on the ventricle surface. The CSF within the

parenchyma is given the material properties of water.

The brain surface is assumed to be mechanically fixed. The top and bottom surface of the slice are impermeable and fixed for displacement along the z-direction, which leads to a quasi 2D situation.

2.3 Diffusion and permeability

The link between diffusion and permeability in brain has not been studied intensively but it seems reasonable to assume that they vary in a similar manner both in amplitude and in direction. In the present study, we assume that the eigen vectors of the diffusion tensor coming from DTI and the CSF permeability inside the parenchyma are the same. Then, the Westhuizen and Du Plessis formula [14] are used for the parallel and perpendicular permeability coefficients of white matter (eqs. 5-6). This formula has been used already by S. Gupta et al. [15] to simulate the three dimensional CSF flow in subarachnoid space (SAS). For the gray matter, isotropic Carman-Kozeny equation [16] is used (eq. 7) to model the laminar CSF flow:

$$k_{para} = \frac{f_0^{\,2}(\pi + 2.157(1-f_0))}{48(1-f_0)^2} d_w^2, [m^2] \quad [5]$$

$$k_{perp} = \frac{\pi f_0 (1-\sqrt{1-f_0})^2}{24(1-f_0)^{3/2}} d_w^2, [m^2] \quad [6]$$

$$k_{gray} = \frac{f_0^{\,3}}{180(1-f_0)^2} d_g^2, [m^2] \quad [7]$$

where, f_0, d_g and d_w are the initial CSF content [0, 1], the distance between gray cell bodies and the diameter of axon fibers, respectively.

Using equations 5 to 7, the permeability coefficients are in a good agreement with the values from literature [5, 6] taking an average CSF content of 18%. In white matter the diameter of fiber tracts falls within the range 1-10 μm [17]. An average of 5 μm is used as an input value for the fiber tract diameter in eqs. 5-6. For the gray matter, the space between the gray cells is also of the order of 5 μm.

The CSF content (f_0) is given by a polynomial regression function of the mean diffusivity (MD). This way, a relationship is established between permeability and diffusion in the brain parenchyma.

3. Isotropic and transverse isotropic (TI) cases

In this section, two different models are introduced to find out the influence of anisotropic permeability in CSF flow. A drained Poisson's ratio of 0.3 is assumed for the solid phase in each case.

3.1 Case 1: isotropic

In this first case, the mechanical properties of the brain are assumed to be isotropic and homogenous. Therefore, the stiffness matrix requires two coefficients, the shear modulus G and the Poisson's ratio ν and the permeability tensor reduces to one scalar coefficient k. The shear modulus is taken from literature and is equal to 3 kPa. The permeability coefficients are taken as the average of all voxel values (eqs. 5-7) over the slice. This way, average permeability and elastic properties of both models are identical.

3.2 Case 2: anisotropic in permeability

In this case, the anisotropy in the permeability tensor is introduced. The elastic properties remain homogenous and isotropic as in case 1. The permeability tensor in the local frame (1,2,3) is obtained using permeability coefficients given by eqs. 5-7. Transverse anisotropy in permeability is introduced in the white matter by the perpendicular and parallel permeability coefficients. The CSF permeability tensors in white and gray matter are written in the local coordinate system (1, 2, 3) (cf. Fig. 1) as follows:

$$\text{Gray matter: } \mathbf{k} = \begin{bmatrix} k_{gray} & 0 & 0 \\ 0 & k_{gray} & 0 \\ 0 & 0 & k_{gray} \end{bmatrix} \quad [8]$$

$$\text{White matter: } \mathbf{k} = \begin{bmatrix} k_{perp} & 0 & 0 \\ 0 & k_{perp} & 0 \\ 0 & 0 & k_{para} \end{bmatrix} \quad [9]$$

4. Results and Discussion

The computed results are presented in this section. The general pattern of displacement in the two cases is very similar. This is not surprising as the mean values of the permeability and elasticity coefficients over the slice are the same for both cases. However, slight differences appear when plotting the dilation (displacement magnitude) versus the arc-length (see Fig. 3) along the left ventricle (distance from a base point on top of the horn of associated ventricle, counter clockwise). Introducing anisotropy in permeability increases the dilation. A similar trend is observed in the right ventricle.

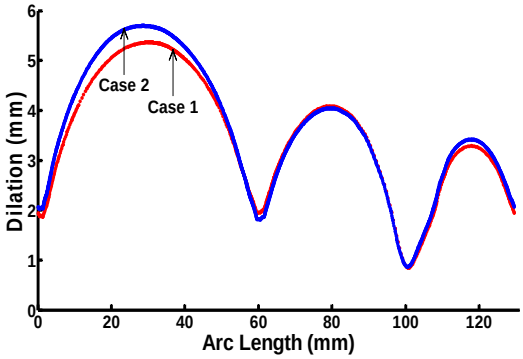

Figure 3. Comparison of the displacement magnitude (mm) in the two cases versus the arc-length (mm) in the left ventricle.

The pressure field is presented in Fig. 4 for case 1 and in Fig. 5 for case 2 together with the streamlines. The effect of introducing anisotropy is clearly visible in Fig. 5. The CSF flow pattern is distorted by anisotropy in case 2. The CSF flows around the fiber directions. The pressure field is also affected by the anisotropic permeability of the parenchyma. It drops when the CSF content increases, as can be seen in the pathways between the two hemispheres.

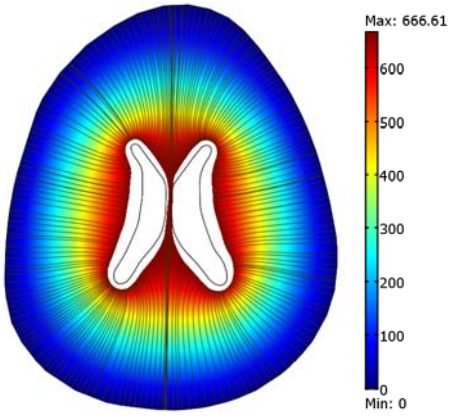

Figure 4. Pressure (Pa) and streamlines of fluid in case 1.

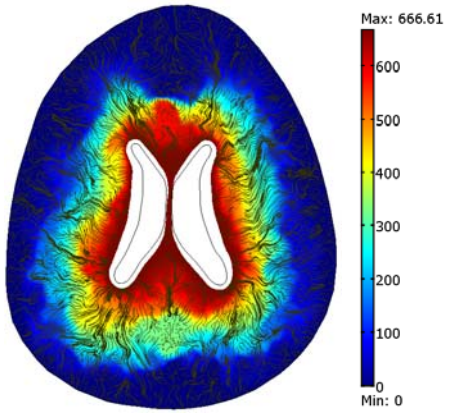

Figure 5. Pressure (Pa) and streamlines of fluid in case 2.

CSF velocity is plotted in a logarithmic scale in Figs. 6-7 for both cases. By introducing anisotropy in case 2, the maximum CSF velocity occurs close to the subarachnoid spaces (SAS) where CSF content is close to 1.0 (high MD). Introducing anisotropy increases the CSF velocity by a factor of ~1000 whereas the ratio between the permeability coefficients along and perpendicular to the fiber tracts direction k_{para} / k_{perp} is only of the order of 100. These permeability coefficients yield a wide range for the CSF velocity going from cm to micron per second. This range has been experimentally observed by Linninger et al. [11]. The CSF pathway close to the SAS and between the two hemispheres shows a large flow of CSF. The increase of CSF velocity is reasonably associated to the high value of CSF content or MD.

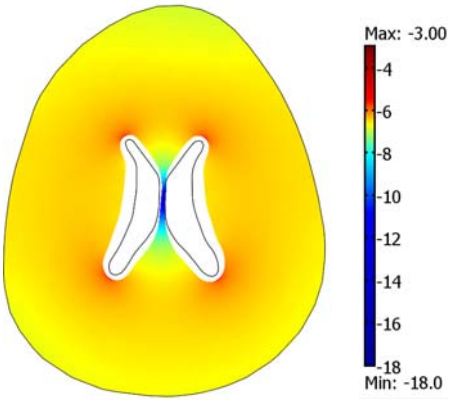

Figure 6. Logarithm of fluid velocity magnitude (m/s) in case 1.

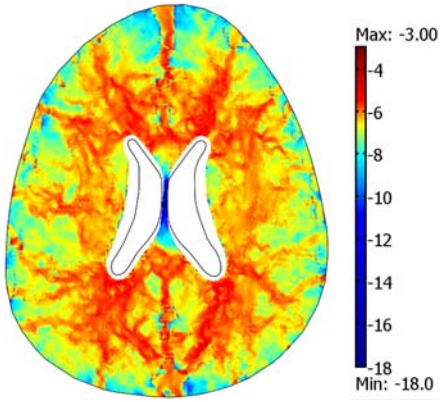

Figure 7. Logarithm of fluid velocity magnitude (m/s) in case 2.

A pressure gradient is imposed in between the ventricles and the SAS as previously done by Momjian and Pena [7, 9]. The existence of such a pressure gradient has never been demonstrated in the case of NPH. Albeit, Levine in his recent study [18] has raised the necessity of the existence of a mini-gradient in the parenchyma. According to him, an increased trans-mantle pressure is needed to balance CSF production and CSF absorption. These aspects will be included in the model.

Due to the incompressibility nature of the brain tissue, the undrained Poisson's ratio is very close to 0.5. In the present study, the drained Poisson's ratio of 0.3 is used to consider the CSF discharge from parenchyma as the ventricles are assumed to be fully permeable. In reality, the CSF flow through the ventricles and the brain membrane is proportional to the difference in pressure on both sides. This aspect is not taken into account in the present model as data are missing.

5. Conclusions

A numerical slice model of one human brain is built in Comsol multiphysics using MRI and DTI data. Experimental voxel based data are imported into Comsol using linear interpolation functions. A transverse isotropic permeability tensor is introduced to model the CSF flow through the brain parenchyma under a given pressure gradient. The computed results clearly show the importance of such anisotropic properties notably in the CSF velocity field.

The model presented here has to be further extended to 3D using MRI technique. Permeability in the brain surface and ventricles has to be introduced as well as sink and source terms to model CSF absorption and production.

Finally, anisotropy in elasticity needs also to be considered in the model. This is planed with the help of the recently developed magnetic resonance elastography (MRE).

6. References

1. A. Peña et al., Communicating hydrocephalus: the biomechanics of progressive ventricular enlargement revisited, *Acta neurochirurgica*, Supplementum **81**, p. 59-63 (2002)

2. T. Nagashima et al., Biomechanics of hydrocephalus: a new theoretical model, *Neurosurgery*, **21**(6), p. 898-904 (1987)

3. S. Hakim and R.D. Adams, The special clinical problem of symptomatic hydrocephalus with normal cerebrospinal fluid pressure: Observations on cerebrospinal fluid hydrodynamics, *Journal of the Neurological Sciences*, **2**(4), p. 307-327 (1965)

4. M.A. Biot, General Theory of Three-Dimensional Consolidation, *Journal of Applied Physics*, **12**(2), p. 155-164 (1941)

5. Sh. Momjian and D. Bichsel, Elastic and Poro-Elastic Models of Ventricular Dilation in Hydrocephalus, *COMSOL Users Conference*, Grenoble (2006)

6. M. Kaczmarek et al., The hydromechanics of hydrocephalus: Steady-state solutions for

cylindrical geometry, *Bulletin of Mathematical Biology*, **59**(2), p. 295-323 (1997)
7. Sh. Momjian and D. Bichsel, Nonlinear poroplastic model of ventricular dilation in hydrocephalus, *Journal of Neurosurgery*, **109**(1), p. 100-107 (2008)
8. T. Dutta-Roy et al., Biomechanical modelling of normal pressure hydrocephalus, *Journal of Biomechanics*, **41**(10), p. 2263-2271 (2008)
9. A. Peña et al., Effects of Brain Ventricular Shape on Periventricular Biomechanics: A Finite-element Analysis, *Neurosurgery*, **45**(1), p. 107 (1999)
10. N. Abolfathi et al., A micromechanical procedure for modelling the anisotropic mechanical properties of brain white matter, *Computer Methods in Biomechanics and Biomedical Engineering*, **12**, p. 249-262 (2009)
11. A.A. Linninger et al., Normal and Hydrocephalic Brain Dynamics: The Role of Reduced Cerebrospinal Fluid Reabsorption in Ventricular Enlargement, *Annals of Biomedical Engineering*, **37**(7), p. 1434-1447 (2009)
12. B. Larrat et al., Anisotropic Viscoelastic Properties of the Corpus Callosum - Application of High-Resolution 3D MR-Elastography to an Alzheimer Mouse Model, *Ultrasonics Symposium IEEE* (2007)
13. E.R. Melhem et al., Diffusion Tensor MR Imaging of the Brain and White Matter Tractography, *American Journal of Roentgenology*, **178**(1), p. 3-16 (2002)
14. J. Vandenwesthuizen and J.P. Duplessis, Quantification Of Unidirectional Fiber Bed Permeability, *Journal of Composite Materials*, **28**(7), p. 619-637 (1994)
15. S. Gupta et al., Three-Dimensional Computational Modeling of Subject-Specific Cerebrospinal Fluid Flow in the Subarachnoid Space, *Journal of Biomechanical Engineering*, **131**(2), 021010-1 (2009)
16. P.C. Carman, Fluid flow through granular beds, *Transactions of the Institution of Chemical Engineers*, **15**, p. 150-166 (1937)
17. Y. Assaf et al., Axcaliber: A method for measuring axon diameter distribution from diffusion MRI, *Magnetic Resonance in Medicine*, **59**(6), p. 1347-1354 (2008)
18. D.N. Levine, Intracranial pressure and ventricular expansion in hydrocephalus: Have we been asking the wrong question?, *Journal of the Neurological Sciences*, **269**(1-2), p. 1-11 (2008)

7. Acknowledgements

The financial support of the STI faculty seed fund at EPF Lausanne is gratefully acknowledged. Prof. Denis Bichsel from Geneva school of engineering is also acknowledged for his helpful collaboration on the Comsol model.